Theor Chem Acc (2010) 126:275–287
DOI 10.1007/s00214-009-0713-y

REGULAR ARTICLE

# The lithium–thiophene interaction: a critical study using highly correlated electronic structure approaches of quantum chemistry

**Michel Caffarel · Anthony Scemama · Alejandro Ramírez-Solís**

Received: 28 October 2009 / Accepted: 30 November 2009 / Published online: 19 December 2009


**Abstract** The fundamental multicentric interaction of a lithium atom with a single thiophene ring is addressed. A systematic study of the interaction energy (IE) and geometry for the Li–T charge-transfer complex is done at the MP2 and CCSD(T) levels using increasingly large basis sets up to aug-cc-pVQZ (AVQZ). Basis set superposition errors (BSSE) are evaluated and shown to have a major impact on the value of the IE. The Fixed-Node Diffusion Monte Carlo (FN-DMC) method is used as an alternative basis-set-free approach to obtain what is likely to be the most accurate estimate of the IE obtained so far. While counterpoise-corrected MP2/AVQZ and CCSD(T)/AVTZ interaction energies are found to be −3.8 and −7.5 kcal/mol, the FN-DMC method yields +1.3 ± 1.7 kcal/mol. The slow convergence of the ab initio IE (and some key structural parameters) with respect to basis set quality and the discrepancy with the FN-DMC result is discussed. A visualization of the electron pairing using the electron pair localization function (EPLF) for the Li-doped versus undoped thiophene is also presented.

**Keywords** Conjugated organic polymers · Polythiophene · Plastic electronics · Quantum Monte Carlo · FN-DMC · CCSD(T) · EPLF

Dedicated to the memory of Professor Jean-Pierre Daudey and published as part of the Daudey Memorial Issue.

M. Caffarel · A. Scemama
Laboratoire de Chimie et Physique Quantiques,
CNRS-IRSAMC Université de Toulouse, Toulouse, France
e-mail: caffarel@irsamc.ups-tlse.fr

A. Ramírez-Solís (✉)
Depto. de Física, Facultad de Ciencias,
Universidad Autónoma del Estado de Morelos,
Cuernavaca, 62209 Morelos, Mexico
e-mail: alex@uaem.mx

## 1 Introduction

Conjugated organic polymers have been extensively studied, both from the experimental and theoretical points of view. They are of practical importance because they combine electronic/optical properties of a semiconductor with the mechanical properties of a conventional plastic material. Furthermore, their properties are easily tuned by chemical modification. In the case of trans-polyacetylene (PA) it has been found experimentally that doping with electron donors or acceptors (D/A) leads to a huge increase in electrical conductivity (for example, [1, 2]) which has been rationalized in terms of the formation of charged solitons [3–6]. One of the crucial points during the doping process is the generation of defects with characteristic distortions of the polymer structure. These defects can be classified as spinless states (charged solitons, bipolarons) and states carrying spin (neutral solitons, polarons). In the case of polymers such as polyparaphenylene, polypyrrole, and polythiophene bipolarons are considered as the spinless charge carriers in these systems (see [7], and references therein). PA has two degenerate ground states, connected through a Peierls transition state, that lead to soliton formation when doped by electron donors or acceptors. Polythiophene (PT) has a non-degenerate ground state where the benzenoid form contains two formal double bonds within the heterocyclic ring (shown schematically in Figure 1(a) of Ref. [8]) is preferred over the quinonoid alternative, with one double bond within the ring plus an inter-ring double bond. Thus, electronic charge transfer due to D/A doping will produce polarons and/or bipolarons rather than solitons. Since PT, as well as its chemical derivatives (e.g. polyethylenedioxythiophene = PEDOT), are well known to be advantageous for many technological applications, it is of considerable interest to examine the

effect of D/A doping on the properties of this prototype polymer. For this reason, one of us participated in a systematic DFT periodic study of the structural and electronic modifications of quasi-1D PT chains when the organic polymer is doped by lithium with varying doping concentrations ($y$ = Li/C atom ratio). In that study [8] the amount of charge transfer from the metal to the chain, the Li–PT bond interaction energy (IE), the carbon–carbon bond length alternation (BLA) pattern which defines the creation of the polaronic/bipolaronic structure, and the band structure evolution as function of the Li doping from $y = 1/4$ to $y = 1/20$ have been addressed. During the calibration stage of this periodic DFT scheme against standard ab initio methods with various basis sets it has been found that most of the geometric parameters of LiT can be readily optimized using relatively simple combinations of correlation treatments (such as MP2) and not-so-large gaussian basis sets. However, quite surprisingly, it was also found that an accurate determination of the Li–T interaction energy is not an easy task and requires the use of rather sophisticated electronic correlation methods coupled with atomic basis sets of very high quality. Also, it has been noticed that the Li–S and both Li–C distances are quite dependent on both the dynamic correlation treatment used and the quality of the basis sets. The basis set issue is so important for the IE that it had already been addressed in Ref. [9] in their SCF and MP2 studies of Na- and Li-doped oligothiophene chains. However, the computational resources then available imposed natural limitations which led them to use basis sets which are very limited by today's standards and only unpolarized basis sets for hydrogen atoms were utilized. For C, S, and Li two types of basis sets were considered: (a) double-zeta (DZ) quality augmented with polarization functions and diffuse $p$ functions on carbon and sulfur and, (b) triple-zeta (TZ) quality augmented by the same additional functions as for the DZ sets. That study showed the crucial importance of polarization functions on lithium and these ranged from $2p$ to $4p1d$ (full details can be found in Table I of Ref. [9]). Although their basis set study was done only on the dithiophene molecule doped with two antifacially located lithium atoms ($Li_2T_2$), it was clear that the MP2 interaction energy varied wildly (from +17.4 to −34.2 kcal/mol) depending on the quality (DZ vs.TZ) of the basis set and on the number and spatial extension of the $p$ and $d$ polarization functions on Li. Another issue that immediately arose was the large basis set superposition error (BSSE), which ranged from −2.1 to −8.1 kcal/mol and significantly modifies the interaction energies with respect to the BSSE-uncorrected ones. However, despite the fact that we were aware of the Li–T interaction energy problem and because the goal of Ref. [8] was to study the band structure of *infinite* periodic Li-doped PT chains, we decided to postpone the investigation of this problem to a later benchmark-type study, which is presented here.

In this work the IE of the Li–T charge transfer complex will be estimated using three different schemes. First, using the second-order perturbational MP2 method with increasingly large basis sets, up to the very large augmented correlation-consistent polarized-VQZ(AVQZ) basis sets of Dunning [10], the geometries being fully optimized with this approach. Second, using the optimized MP2 geometries with each basis set, by applying the very accurate CCSD(T) method up to the large augmented correlation-consistent polarized-VTZ(AVTZ) basis set, which represents our computational limit. As mentioned above, given the importance of the BSSE errors, the counterpoise correction to both of these ab initio energies is applied. At this point we stress that there is a strong electron transfer from the lithium atom to the thiophene ring; the first estimation (given by Irle and Lischka [9]) is between 0.6 and 1 electron and a HF Natural Population Analysis (nearly basis set independent) with the aug-cc-pVTZ basis set [10] yields a large transfer of 0.88 electron at the corresponding optimized MP2 geometry.

Finally, since the Li–T interaction energy seems to be much dependent on both the basis set quality and on the nature of the electronic correlation treatment, we have performed Fixed-Node Diffusion Monte Carlo calculations (FN-DMC) which, by its very nature, does not contain any BSSE and is completely free of the electronic excitation-degree correlation problem. Taking into consideration that the ground-state wavefunction of LiT is essentially mono-configurational, the fixed-node error (the only residual systematic error of FN-DMC when statistical fluctuations have been sufficiently reduced) is expected to be rather small. As a consequence, the FN-DMC calculation of the IE presented here should be considered as a benchmark value.

From the physical point of view the Li–T interaction is quite complex for three reasons: (a) Since Li transfers charge to the T ring, the latter will become negatively charged and this fact requires particular attention similar to the calculation of electron affinities (see e.g., [11]). (b) Since Li is simultaneously adjacent to the five atomic centers of the ring, the Li–T interaction implies dynamic correlation effects involving pairs, triplets, and quartets of orbital interactions on two, three, and four atoms. This is similar to the complex interactions of metal atoms when they are coordinated to cyclopentadienyl. These three- and four-center interactions imperatively require the use of very sophisticated electronic correlation schemes if one aims at obtaining truly accurate interaction energies. (c) Isolated thiophene contains two formal double CC bonds and one central CC single bond. The natural charge transfer that occurs from the metal to the ring induces

significant carbon–carbon bond distance rearrangements, thus leading to an inversion of the BLA pattern in the ring as the Li atom approaches its equilibrium geometry. However, these BLA modifications are two-way coupled to the extent of metal-to-ring charge transfer, thus closely relating this point with (a).

We note that, at the equilibrium geometry of the LiT molecule, the CASSCF(3,4) wavefunction is largely dominated by the Hartree–Fock determinant with a CI coefficient of 0.97. It is important to emphasize that larger active spaces do not modify this fact and this picture is practically independent of the basis set quality. Since the HF determinant is largely dominant the open-shell unrestricted MP2 method can, in principle, provide good estimates of the IE. However, Coupled Cluster calculations at the CCSD(T) level using the largest possible atomic basis sets, is undoubtedly the best approach if one wishes to obtain benchmark-type quality ab initio interaction energies.

In this study we also propose to visualize the electron-pairing occurring in this system. In standard computational chemistry several approaches have been developed to analyze and visualize the electronic distribution in the ordinary 3D-space. Among them we can cite, e.g., the methods analyzing the deformation of densities (a build-up of charge between two atoms is interpreted as the existence of a bond) [12], the methods based on the topological analysis of the electron density or its Laplacian (see, for instance, Bader [13]), the methods studying the topography of the molecular electrostatic field [14] and, also, approaches using as indicator the electron localization function (ELF) describing the amount of local Pauli repulsion between electrons [15, 16]. Of course, this list cannot be considered as exhaustive since defining a successful and general qualitative model for the description of chemical structure is an everlasting theme in chemistry since the pioneering electron-pair model of Lewis.

In this work we propose to exploit the accurate data obtained from our FN-DMC simulations to get some insight into the electron localization properties of the LiT molecule at its equilibrium geometry. To do that we shall use the function, introduced by some of us [17], describing the pairing of electrons in a molecular system. This function, called electron pair localization function (EPLF), is built to reveal the differences in the average distances between spin-like and spin-unlike electrons. In regions where localized pairs of electrons are present (lone pairs, atomic pairs, bonds) the EPLF takes large values and displays maxima. In contrast, in regions where electrons behave essentially as an homogeneous fluid (spin-like and spin-unlike electrons being mixed together), the EPLF takes much smaller values. The form of the EPLF is simple and has been chosen to be easily computable using quantum Monte Carlo (QMC) calculations. Originally applied to several simple atomic and molecular systems [17], the EPLF has recently proven to be a practical tool for describing electronic features in more complex molecular systems [18, 19]. It is applied here to our challenging chemical problem involving subtle changes in electron pairing upon Li doping of the thiophene ring.

The organization of the paper is as follows. In Sects. 2 and 3 the electronic structure approaches used in this study [MP2 and CCSD(T) on the one hand and QMC approaches on the other hand] are briefly presented. In particular, for the ab initio approaches the choice of the gaussian basis sets employed is discussed and the very basic features of QMC needed to understand the present work are briefly summarized. In Sect. 4 the Electron Pair Localization Function (EPLF) is presented. A few computational details are given in Sect. 5, and our numerical results including the EPLF visualization of the electronic pairings are presented in Sect. 6. Finally, a summary of this study is given in the last section, Sect. 7.

## 2 Dynamic correlation treatment using MP2 and CCSD(T): choice of the atomic basis set

In [8] one of us has shown that the LiT open-shell molecule can be very well described at the zeroth-order by the Hartree–Fock wavefunction. Since both Li and LiT are open-shell systems we shall use here the unrestricted open-shell formalism for these species, which then can be extended to the UMP2 and UCCSD(T) methods to account for the dynamic electronic correlation effects. For the thiophene molecule we use the restricted versions, namely the RMP2 and the RCCSD(T) methods. The optimized geometries of the isolated thiophene (T) and the LiT complex were obtained using the 2nd-order perturbational Möller–Plesset scheme (MP2) as programmed in the Gaussian03 code [20].

As mentioned earlier, the calculation of the Li–T interaction energy could, at first sight, seem to be a simple and straightforward task. However, since the pioneering work Irle and Liscka [9] where the dilithium–dithiophene ($Li_2T_2$) interaction energy was studied, it became clear that the choice of the optimal basis sets to achieve this task is far from being obvious. This problem arises mainly because the extent to which charge transfer occurs from Li to T is strongly coupled to the charge delocalization (leading to the BLA changes) on the ring backbone and vice-versa. Thus, we will approach this IE problem in an incremental manner using increasingly large basis sets with both correlated methods; these were applied to all atoms and comprise the 6-31G**, 6-311G*, 6-311+G**, aug-cc-pVDZ (AVDZ), aug-cc-pVTZ (AVTZ) and up to the very large aug-cc-pVQZ (AVQZ) [10] basis sets. These lead to

108, 128, 164, 178, 372, and 668 molecular orbitals in the LiT case, respectively. The MP2 optimizations of T and LiT could be performed using the huge AVQZ basis set,[1] but the CCSD(T) calculation on LiT could not be achieved due to computational (disk) limitations. Given that the Basis Set Superposition Error (BSSE) is crucial for our purpose here, we shall also report BSSE-corrected CCSD(T) interaction energies.

## 3 Dynamic correlation treatment using Variational Monte Carlo (VMC) and Fixed-Node Diffusion Monte Carlo (FN-DMC)

In view of the great sensitivity of the ab initio results as a function of the size of the basis set used it is particularly important to call for alternative electronic structure approaches which are much less dependent on the nature of the basis set but are still capable of giving the major part of the dynamical correlation contribution. Here, we propose to use the quantum Monte Carlo approach which is particularly powerful when dynamical correlation effects are searched for. QMC methods are stochastic methods and are fundamentally different from the commonly used deterministic approaches based either on the expansion of the wavefunction on a set of antisymetrized products of one-electron molecular orbitals (post-HF methods) or on the use of the electronic density via appropriate exchange-correlation energy functionals (DFT approaches). In a few words, a quantum Monte Carlo algorithm can be viewed as a molecular-dynamics-type approach applied to the electrons (not the nuclei!) in which an additional stochastic step is introduced (Monte Carlo step). From a practical point of view, a quantum Monte Carlo scheme can be viewed as an algorithm generating by a step-by-step procedure (time evolution) a series of "states" or "configurations". Here, a configuration is defined as the set of the $3N$-electronic coordinates ($N$ number of electrons), the positions of the nuclei being fixed (Born-Oppenheimer condition)

$$\vec{R} = (\vec{r_1}, \ldots, \vec{r_N}) \tag{1}$$

Stated differently, a configuration $\vec{R}$ may be viewed as a "snapshot" of the molecule showing the instantaneous positions of each electron. Stochastic and deterministic rules are chosen so that configurations are generated in average according to some target probability density, $\Pi(\vec{R})$. Note that the probability density is defined over the complete $3N$-dimensional configuration space and not over the ordinary 3D-space. Many variants of QMC can be found in the literature (referred to with various acronyms: VMC, DMC, PDMC, GFMC, etc...). They essentially differ by the type of stochastic rules used and/or by the specific stationary density produced. In practice, the two most popular QMC approaches used for simulating complex molecular systems are the so-called Variational Monte Carlo (VMC) and Fixed-Node Diffusion Monte Carlo (FN-DMC) methods. Both methods will be employed here and in what follows only the very basic features useful for understanding this work are given (for a detailed presentation, see, e.g. [21]).

### 3.1 Variational Monte Carlo (VMC)

In a VMC calculation the probability density generated is given by

$$\Pi_{\mathrm{VMC}}(\vec{R}) = \frac{\psi_T^2(\vec{R})}{\int \mathrm{d}\vec{R}\psi_T^2(\vec{R})} \tag{2}$$

where $\psi_T$ is a high-quality electronic trial wave function. A commonly used expression for $\psi_T$ consists of a product of two terms. The first term is standard and is introduced to describe the one-particle shell-structure of molecules. It is obtained from a preliminary HF or DFT ab initio calculation and is expressed as one (or a combination of a few) determinant(s) of single-particle spatial orbitals. The second term is introduced to reproduce the electron–electron cusp condition of the exact wave function and, also, to incorporate some explicit coupling between electron–nucleus and electron–electron coordinates (see, [22]). Note that the electron–electron cusp condition is known to be particularly difficult to fulfill in standard ab initio calculations using expansions over one-electron basis sets (necessity of considering very high values of the orbital momentum). The explicitly correlated term is usually referred to as the Jastrow factor. In a spin-free formalism our trial wave function is written as

$$\psi_T(\vec{R}) = D^{\uparrow}(\vec{R})D^{\downarrow}(\vec{R}) \exp\left[\sum_{\alpha}\sum_{\langle i,j\rangle} U(r_{i\alpha}, r_{j\alpha}, r_{ij})\right] \tag{3}$$

where the sum over $\alpha$ denotes a sum over the nuclei, $\sum_{\langle i,j \rangle}$ a sum over the pair of electrons, and $D^{\sigma}$ ($\sigma = \uparrow$ or $\downarrow$) are determinants made of one-particle space-orbitals and $U$ is the Jastrow factor. Different expressions for the Jastrow part have been presented in the literature. Here we have chosen a form presented in detail in Ref. [23].

A critical step in a VMC approach is the optimization of the parameters entering the trial wave function. A standard method consists in searching for parameters minimizing

[1] To give an idea of the computational resources required with the largest basis set, the MP2/AVQZ optimization of LiT used more than 150 GB of disk space, 27 GB of RAM and took 5 days on 8 processors starting from the MP2/AVTZ optimized geometry.

the fluctuations in configuration space of the local energy defined as

$$E_L(R) = H\Psi_T(R)/\Psi_T(R) \tag{4}$$

This criterion is based on the fact that for the exact wave function the local energy reduces everywhere to a constant—the exact energy—and, thus, the fluctuations of the local energy entirely vanish. Accordingly, small fluctuations are associated with "good" trial wave functions. A number of methods have been developed to perform efficiently the optimization step within a QMC framework. In this work, we have used the correlated sampling method of Umrigar et al. [24], an approach based on the minimization of the weighted variance of the local energy over a set of fixed configurations.

Once the optimal parameters have been determined, the quality of the resulting trial wave function is usually good. A major part of the dynamical correlation energy (Coulomb hole) is recovered and the *gross* features of the one-particle background are also correctly described via the determinantal part (i.e., the non-dynamical correlation). For most atoms it is possible to recover up to 80–90% of the exact correlation energy [22]; for molecules, the domain of variation lies usually between 30 and 90%.

The numerical method (stochastic rules) employed to generate the VMC density, Eq. 2, is standard. It is based on the use of an improved Metropolis algorithm [25].

### 3.2 Fixed-Node Diffusion Monte Carlo (FN-DMC)

In a diffusion Monte Carlo scheme the stochastic rules employed are the same as in the VMC case (Metropolis algorithm) plus a new rule corresponding to a branching (or birth-death) process. More precisely, depending on the magnitude of the local energy a given configuration is destroyed (when the local energy is greater than some estimate of the exact energy) or duplicated a certain number of times (local energy lower than the exact energy). It can be shown that the stationary density resulting from these rules is now given by

$$\Pi_{\mathrm{DMC}}(\vec{R}) = \frac{\psi_T(\vec{R})\phi_0(\vec{R})}{\int \mathrm{d}\vec{R}\psi_T(\vec{R})\phi_0(\vec{R})} \tag{5}$$

where $\phi_0(\vec{R})$ denotes the ground-state wave function.

*Fixed-node error* Actually, because the density $\Pi_{\mathrm{DMC}}$ is necessarily positive, as any stationary density resulting from some stochastic rules, $\phi_0$ is not the exact ground-state wave function, but some approximate one resulting from the additional constraint that $\phi_0$ must have the same sign as the trial wave function so that the product in Eq. 5 is always positive. In other words, the mathematical eigenproblem solved is not the exact one but, rather, some modified one which can be written as

$$H\phi_0^{\mathrm{FN}}(\vec{R}) = E_0^{\mathrm{FN}}\phi_0^{\mathrm{FN}}(\vec{R}) \tag{6}$$

where $\phi_0^{\mathrm{FN}}(\vec{R}) = 0$ whenever $\psi_T(\vec{R}) = 0$.

The fact that the nodes (points in $3N$-dimensional space where the wave function vanishes) of $\psi_T$ and $\phi_0^{\mathrm{FN}}$ are identical leads to a so-called "fixed-node" error. However, as far as total energies are concerned, this approximation is in general very good and the fixed-node error on total energies represents usually a small fraction of the total correlation energy. Let us emphasize that this error depends only on the quality of the nodes; see, e.g., the discussion in [26]). In the context of this work it is quite interesting to note that a benchmark-type study by Grossman [27] (see, also the study by Manten and Lüchow, Ref. [28]) on the calculation of the atomization energy of 55 molecules (G1 set of Pople and collaborators [29]) has shown that by using FN-DMC simulations with Hartree–Fock nodes the quality of the results was quite high and similar to that obtained with the CCSD(T) method with large basis sets.

## 4 The electron pair localization function (EPLF): a tool for visualizing electronic pairings

The EPLF is a local scalar function defined in the ordinary 3D-space, bounded above and below, which focuses essentially on the localization of electron *pairs*. It is a good descriptive tool for chemical bonds, since pairs of electrons play a central role in our everyday interpretation of chemical structure and reactivity (Lewis model, VSEPR). The framework proposed to calculate such a localization function is that of quantum Monte Carlo approaches. As emphasized in the introduction, QMC are techniques of a great versatility and, therefore, the definition of the EPLF proposed below will be of practical use for any type of wavefunctions (HF, post-HF, Valence Bond, etc...) and for any level of computation (VMC, FN-DMC,"exact").

First, we need to introduce the two local quantities $d_{\sigma\sigma}(\vec{r})$ and $d_{\sigma\bar{\sigma}}(\vec{r})$ defined as follows:

$$\begin{aligned} d_{\sigma\sigma}(\vec{r}) &\equiv \sum_{i=1}^{N} \langle\langle \delta(\vec{r}-\vec{r}_i) \min_{j;\ \sigma_j=\sigma_i} |\vec{r}_i - \vec{r}_j| \rangle\rangle \\ d_{\sigma\bar{\sigma}}(\vec{r}) &\equiv \sum_{i=1}^{N} \langle\langle \delta(\vec{r}-\vec{r}_i) \min_{j;\ \sigma_j\neq\sigma_i} |\vec{r}_i - \vec{r}_j| \rangle\rangle \end{aligned} \tag{7}$$

where $\{\vec{r}_k\}_{k=1,N}$ are the positions of the $N$ electrons for a given configuration $\vec{R}$, $\sigma_i$ is the spin of the $i$th electron ($\sigma_i = \uparrow, \downarrow$), and $\langle\langle \ldots \rangle\rangle$ the stochastic average over the Monte Carlo configurations. As seen from these definitions $d_{\sigma\sigma}(\vec{r})$ [resp., $d_{\sigma\bar{\sigma}}(\vec{r})$] is the average distance between an electron

located at $\vec{r}$ and the closest spin-like (resp., spin-unlike) electron of the molecule.

The EPLF is defined as

$$\mathrm{EPLF}(\vec{r}) = \frac{d_{\sigma\sigma}(\vec{r}) - d_{\sigma\bar{\sigma}}(\vec{r})}{d_{\sigma\sigma}(\vec{r}) + d_{\sigma\bar{\sigma}}(\vec{r})} \tag{8}$$

Figure 1 of [17] gives a simple pictorial representation of the construction of the EPLF in the case of only one configuration and four electrons in 2D.

By definition the EPLF takes its values within the interval $[-1,1]$. It gives a local indicator of electron pairing as follows. In regions of space where electrons are unpaired the average distances between spin-like and spin-unlike electrons are similar, $d_{\sigma\bar{\sigma}} \approx d_{\sigma\sigma}$, and the EPLF goes to zero. When spin-unlike electrons are paired we have $d_{\sigma\bar{\sigma}} \ll d_{\sigma\sigma}$ and EPLF goes to 1. Finally, when spin-like electrons are paired, $d_{\sigma\bar{\sigma}} \gg d_{\sigma\sigma}$ and, thus, EPLF goes to $-1$. The EPLF main feature is to reveal the differences in the average distances between spin-like and spin-unlike electrons. In regions where localized pairs of electrons are present (lone pairs, atomic pairs, bonds) the EPLF takes larger values and displays maxima. In contrast, in regions where electrons behave essentially as an homogeneous fluid (spin-like and spin-unlike electrons being mixed together), the EPLF takes much smaller values. In particular, note that for molecules with one or more open shells, in regions where there is a larger amount spin-up (or spin-down) density, by construction the EPLF takes on minima values. Note that the definition of EPLF is particularly well suited to QMC; the formula (7) can indeed be easily computed with any QMC scheme.

## 5 Computational details

### 5.1 Basis sets and nuclear geometries for the QMC calculations

As already mentioned, the atomic gaussian basis functions used for all atoms are the fully decontracted Dunning aug-cc-pVTZ basis sets [10]. The MP2/AVTZ optimized geometries for the isolated thiophene and the LiT complex have been used.

### 5.2 QMC simulations

Since the HF wavefunction is an excellent zeroth-order approximation for the Li atom, the thiophene, and the LiT molecules, the trial wavefunctions used here for the FN-DMC simulations consist of the RHF(T) or UHF(Li, LiT) determinants multiplied by a standard Jastrow prefactor taking into account the explicit electron–electron and electron–electron–nucleus interactions (see, e.g. [30, 31]). Note that for a system consisting of light atoms such as C, H, and S some care has to be taken for properly reproducing the electron–nucleus cusp both for the core and valence electrons. Regarding the core region, we have replaced the $1s$ atomic orbitals of the carbon and sulfur atoms expanded over the gaussian basis set by the $1s$ Slater-type orbital given in the Clementi and Roetti's Tables [32]. On the other hand, the valence molecular orbitals are also modified at short nuclear distances to impose the nuclear cusp; we do that by using a short-$r$ representation of the radial part of orbitals under the form $c_1\exp(-\gamma_1 r) + c_2 r^2 \exp(-\gamma_2 r)$, in the same spirit as Ref. [33]. The present FN-DMC calculations are all-electron calculations done with a very small time-step, $\tau = 8 \times 10^{-5}$, to insure a proper treatment of the nodal hypersurfaces and to reduce time-step errors. For each trial wave function and for each atomic (Li) and molecular systems (T and LiT), the calculations are very extensive and represent more than $10^{10}$ Monte Carlo steps distributed over a large number of processors (around one hundred).

### 5.3 EPLF data

The continuous 3D-space is represented using a $80 \times 80 \times 80$ three-dimensional grid. The EPLF is calculated as follows: for each Monte Carlo configuration generated the positions of the electrons are scanned. The elementary volume of the 3D-grid occupied by each electron is determined and the minimum distances appearing in the definition of EPLF are calculated. The noise in the localization function due to the statistical character of QMC simulations has been reduced by using a median blur filter as detailed in Ref. [17]. This filter is particular well adapted here since it is known to modify very little the regions where the gradient is large. This latter point is particularly important here since we are interested in altering as little as possible the contours of the pair localization function.

## 6 Results

### 6.1 The geometry of the Li–thiophene complex

For thiophene and for the Li–thiophene charge-transfer complex, MP2 geometry optimizations have been performed with all the basis sets. For thiophene, the CC and CS bond distances computed by the SCF method are improved consistently by electron correlation effects and the final MP2 results agree very well with experimental data [34]. The computed CH bond distances evaluated at the SCF level are already very close to the experimental ones. Note that the original MP2 CH distances reported by Irle and Lischka [9] overshoot the experimental ones by

**Table 1** MP2 optimized geometries for thiophene and for the LiT complex as functions of the atomic basis set employed; distances in angstroms and angles in degrees

| | 6-31G (108)** | 6-311G (128)* | 6-311+G (164)** | AVDZ (178) | AVTZ (356) | AVQZ (668) |
|---|---|---|---|---|---|---|
| Thiophene | | | | | | |
| S1–C2 | 1.715 | 1.713 | 1.713 | 1.729 | 1.716 | 1.704 |
| C2–C3 | 1.377 | 1.381 | 1.382 | 1.391 | 1.378 | 1.376 |
| C3–C4 | 1.419 | 1.421 | 1.421 | 1.427 | 1.413 | 1.411 |
| BLA | 0.042 | 0.040 | 0.039 | 0.036 | 0.035 | 0.035 |
| C5S1C2 angle | 91.99 | 92.13 | 92.14 | 92.07 | 92.32 | 92.49 |
| C2C3C4 angle | 112.37 | 112.26 | 112.23 | 112.46 | 112.49 | 112.43 |
| Li–thiophene | | | | | | |
| S1–C2 | 1.773 | 1.771 | 1.771 | 1.792 | 1.767 | 1.759 |
| C2–C3 | 1.428 | 1.432 | 1.431 | 1.437 | 1.424 | 1.421 |
| C3–C4 | 1.393 | 1.395 | 1.394 | 1.402 | 1.389 | 1.386 |
| BLA | −0.035 | −0.037 | −0.037 | −0.035 | −0.035 | −0.035 |
| C5S1C2 angle | 89.86 | 90.16 | 90.15 | 89.89 | 90.25 | 90.47 |
| C2C3C4 angle | 112.89 | 112.87 | 112.88 | 113.13 | 113.07 | 113.02 |
| Li–S1 | 2.609 | 2.549 | 2.545 | 2.582 | 2.546 | 2.540 |
| Li–C2 | 2.153 | 2.130 | 2.128 | 2.163 | 2.138 | 2.137 |
| Li–C3 | 2.189 | 2.187 | 2.189 | 2.229 | 2.185 | 2.181 |
| S1C2C3C4 dihedral | 17.22 | 16.31 | 16.33 | 16.39 | 15.52 | 15.48 |

BLA stands for Bond Length Alternation (see text for the definition). Ring site numbering starts clockwise on the sulphur atom (S1) and ends on the last carbon on the left (C5) of the ring. The number of uncontracted atomic functions corresponding to each basis set for LiT is indicated in parentheses

about 0.01 Å; this is due to the fact that polarization functions on the hydrogen atoms were not used at that time for computational limitations. Since we are mainly interested in the geometry changes of the ring systems, we did not see any need to improve further the C–H bonds. Calculated bond angles agree very well with experimental ones. Table 1 shows the evolution of the main geometrical parameters, namely the single and double CC bonds for the thiophene and LiT molecules as functions of the basis set quality. The BLAs, commonly defined as the difference between these two CC distances, are also given. Note that the geometry changes in the thiophene ring induced by the interaction with the Li atom anticipate the quinonoid structures found in the higher PT oligomers.

Clearly, for the isolated thiophene molecule the MP2 geometrical parameters (distances and angles) show a rather fast convergence with respect to basis set quality. This is particularly important for the convergence of the BLA (defined previously), which in the PT polymer is the crucial geometrical parameter related to changes in the non-linear optical properties [6, 7]. However, note that even for isolated thiophene, the AVDZ basis shows some anomalous behavior, leading to slightly larger S1-C2, C2-C3, and C3-C4 bond lengths than those obtained with the smaller basis sets; in particular, the C2-C3 and C3-C4 distances obtained with the AVTZ basis set are even smaller than those of the 6-311+G** basis set.

As it is well-known, when the Li atom interacts with thiophene the charge transferred from the metal to the ring induces an inversion of the BLA, that is, the original CC double bonds of thiophene become "single bonds" while the single CC bond acquires some "double bond" character. Three crucial geometrical facts related to the discussion of the IE must be pointed out: (a) the MP2 optimizations performed with different basis sets, although also leading to nearly constant BLA values around −0.035 Å, actually yield different C2-C3 and C3-C4 distances, (b) the distances of the Li atom to the three different sites (Li–S1, Li–C2, Li–C3) on the ring show larger variations (0.03–0.04 Å) with respect to basis set quality, in particular when going from AVDZ to AVTZ. (c) in all cases, the Li atom is closer to the pair of carbon atoms adjacent to the sulphur site, but the difference between the Li–C2 and Li–C3 distance also oscillates with respect to basis set quality. The C5S1C2 and C2C3C4 optimized angles are practically independent of basis set quality. As always, it would be desirable to achieve basis set convergence of the molecular properties; in this direction the next natural step would be to obtain results with the even larger aug-cc-pV5Z basis sets. However, note that the MP2/AVQZ

**Table 2** Total energies (a.u.) using the MP2 and CCSD(T) approaches as a function of the atomic basis set employed

| | 6-31G (108)** | 6-311G (128)* | 6-311+G (164)** | AVDZ (178) | AVTZ (356) | AVQZ (668) |
|---|---|---|---|---|---|---|
| MP2 | | | | | | |
| Li | −7.431235 | −7.432026 | −7.432027 | −7.432425 | −7.432705 | −7.432718 |
| T | −551.948437 | −552.007218 | −552.044170 | −552.018724 | −552.208032 | −552.269648 |
| LiT | −559.376948 | −559.442097 | −559.479422 | −559.469513 | −559.647414 | −559.709108 |
| $D_e$ | 1.71 | −1.79 | −2.02 | −11.52 | −4.19 | −4.23 |
| LiT(BSSE) | −559.367049 | −559.433185 | −559.473034 | −559.450940 | −559.645948 | −559.708499 |
| $D_e^{BSSE}$ | 7.92 | 3.80 | 1.98 | 0.13 | −3.27 | −3.84 |
| CCSD(T) | | | | | | |
| Li | −7.431235 | −7.432030 | −7.432026 | −7.432425 | −7.432679 | – |
| T | −552.012998 | −552.070265 | −552.109046 | −552.084168 | −552.276634 | – |
| Li + T | −559.444233 | −559.502291 | −559.541072 | −559.516593 | −559.709313 | – |
| LiT | −559.446748 | −559.511059 | −559.550114 | −559.526816 | −559.722438 | – |
| $D_e$ | −1.58 | −5.50 | −5.67 | −6.41 | −8.23 | – |
| LiT(BSSE) | −559.437238 | −559.502312 | −559.543821 | −559.523628 | −559.721271 | – |
| $D_e^{BSSE}$ | 4.39 | −0.01 | −1.72 | −4.41 | −7.50 | – |

The number of atomic functions corresponding to each basis set is indicated in parentheses. The interaction energies $D_e$ and their BSSE-corrected values are given in kcal/mol

calculations are already at the limit of what can be achieved with present day computational resources, so that even the corresponding CCSD(T)/AVQZ calculations are out of reach.[2] Keeping in mind these facts, we proceed to the energetic analysis of the Li–T interaction.

### 6.2 MP2 and CCSD(T) ab initio interaction energies (IE) and BSSE corrections

Table 2 shows the total energies for LiT and the isolated fragments (Li atom and the thiophene molecule at the MP2 optimized geometries), and the interaction energies of the Li–T system using the MP2 and CCSD(T) approaches as a function of the basis set employed. The basis-set-superposition-error (BSSE)-corrected interaction energies are also given. Several interesting facts can be highlighted from this table. First of all, like in the previous study by Irle and Lischka for dilithium–dithiophene, we find that the BSSE-uncorrected interaction energies at the MP2 level vary quite a lot depending on the quality of the basis set, from +1.71 kcal/mol to −11.5 kcal/mol. Also, it is somewhat surprising that the largest MP2 BSSE-uncorrected IE is found for the AVDZ basis set instead of the AVQZ one. Nevertheless, when the BSSE correction is applied, the expected monotonic increase for the MP2 interaction energy is recovered as the basis set quality improves; note that the range of BSSE-corrected MP2 energies is nearly as large as that of the uncorrected energies, but the BSSE decreases dramatically from 11.65 kcal/mol for the AVDZ basis set to only 0.92 and 0.39 kcal/mol at the MP2/AVTZ and MP2/AVQZ levels, respectively. This result might be related to the previously mentioned geometrical anomalies found for the LiT complex when described with the AVDZ basis set. We stress that only with the very large AVTZ and AVQZ basis sets the Li–T complex becomes slightly stable at the MP2-BSSE level of theory. These results show again the utmost importance of the most diffuse radial orbitals as well as the essential role of the higher-angular momentum functions to address this complex multicentric interaction. When analyzing the corresponding results at the CCSD(T) level, two qualitative changes with respect to the MP2 results appear immediately: (a) all the BSSE-uncorrected IE are negative (attractive) and the range in which they vary is smaller, from −1.6 to −8.2 kcal/mol; (b) an increasingly attractive monotonic behavior is observed with respect to basis set quality, even without the BSSE correction. When the BSSE correction is applied, a systematic decrease in the IE is observed and, as could be expected, this correction gets smaller (from almost 6 kcal/mol with 6 −31G** to only 0.73 kcal/mol with AVTZ) with increasing basis set quality.

Finally, let us conclude this section about ab initio results by saying that, although the CCSD(T) approach can be probably considered as one of the most reliable ab initio methods when multi-configurational effects are negligible and when large basis sets are used, it is clear that the results obtained here are far from being satisfactory and definitive. The final value of (at least) 7.5 kcal/mol for the binding

[2] The CCSD(T)/AVTZ calculations for LiT already involve about $1.5 \times 10^7$ CSF.

energy of the Li–T charge transfer complex must be taken with lot of care, since a large variation of more than 3.1 kcal/mol still appears when going from CCSD(T)/AVDZ to CCSD(T)/AVTZ including BSSE; this represents a rather large (70%) increase in the BSSE-corrected CCSD(T) interaction energy, clearly showing that results with much larger basis sets are still needed to apply any extrapolation technique.

### 6.3 QMC results

Given the large variations found with both ab initio methods for the Li–T interaction energy, we decided to perform Fixed-Node Diffusion Monte Carlo (FN-DMC) simulations. The geometries used are those obtained at the MP2/AVTZ level both for the isolated thiophene and for the LiT complex.

Figure 1 shows the evolution of the FN-DMC interaction energy as a function of the number of Monte Carlo (MC) steps. Let us emphasize that the number of MC steps is proportional to the CPU time needed to perform the calculation and is therefore a direct indicator of the computational effort. As it can be seen, the simulations are quite intensive: the maximum number of MC steps done here is about $2 \times 10^{10}$ for the separate fragments as well as for the LiT complex. To perform such a large number of steps, we exploit the maximal efficiency of QMC approaches with respect to parallel computations (any QMC simulation of length $L$ can be divided into $P$ shorter and *independent* simulations of length $L/P$). Typically, the calculations presented in this work have been done using 64 or 128 processors. By looking at the convergence of the IE as a function of the simulation time, it is clear that to get converged results a quite large amount of computation is needed. To be more precise, at up to $4 \times 10^9$ MC steps we are still in the transient regime where the IE mean value displays a systematic drift in time. Only after this regime has passed the stationary domain is reached, and the IE is almost stabilized within a couple of kcal/mol.

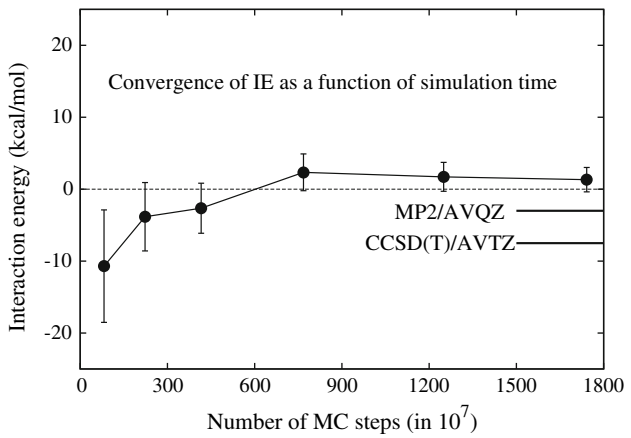


**Fig. 1** Convergence of the interaction energy computed with FN-DMC as a function of the number of Monte Carlo steps

**Table 3** Total and interaction energies of the Li–T system at the HF, CCSD(T)/AVTZ, and FN-DMC levels

| | Hartree–Fock | CCSD(T)/AVTZ | FN-DMC |
|---|---|---|---|
| Li | −7.43268 | −7.43268 | −7.47779(5) |
| T | −551.37996 | −552.27663 | −552.9157(17) |
| Li + T | −558.81264 | −559.70931 | −560.3929(17) |
| LiT | −558.79460 | −559.72244 | −560.3908(20) |
| $D_e$ (kcal/mol) | +11.34 | −8.23 | +1.3 ± 1.7 |

All energies in atomic units, unless otherwise stated

Table 3 shows the final FN-DMC results obtained with our most extensive simulations. For the sake of comparison, we also present the Hartree–Fock as well as the CCSD(T) values obtained with the largest basis set (no BSSE corrections are reported since we just want to compare total energies). As seen in the table, the total energies obtained with FN-DMC are excellent and, in any case, much better (lower) than the CCSD(T)/AVTZ values. For the Li atom, knowing that the total correlation energy is estimated to be 0.04533 a.u.(e.g., Ref. [35]) we see that the FN-DMC calculation recovers about 99.5 ± 0.1% of the correlation energy, which is of course an excellent result. Note that in the case of the CCSD(T) calculation for this three-electron system and, because we are in the approximation where two electrons are kept fixed in the innermost 1*s* atomic orbital, the CCSD(T) result is expected to converge to the Hartree–Fock result and this is indeed what is observed. For the thiophene and the Li–thiophene systems the FN-DMC are much lower than the CCSD(T) results. For example, in the thiophene case the total energy at the CCSD(T) level is lower than the HF energy by about 0.9 a.u, while at the FN-DMC level the energy value is lower than the CCSD(T) one by an additional amount of about 0.6 a.u. Similar results are obtained for other systems. These results, which are rather impressive, are cleary in favor of FN-DMC. However, to be fair, some caution is needed here. Indeed, using a FN-DMC scheme the core electrons are automatically correlated (they are part of the all-electron simulations). In constrast, this is not the case for the CCSD(T) calculations performed by using (very) large basis sets and by freezing the core electrons to avoid huge and untractable Hilbert spaces. As a consequence, the frozen-core CCSD(T) total energies are significantly higher than in the FN-DMC case. Various comparative studies, e.g. [27, 28], have shown that CCSD(T) and FN-DMC calculations are of a much more similar quality when atomic cores play only a marginal role (for example, when computing *differences* of molecular energies).

Now, it is important to comment in some detail the disagreement observed between the FN-DMC interaction energy of $+1.3 \pm 1.7$ kcal/mol and the ab initio BSSE-corrected CCSD(T)/AVTZ value of $-7.5$ kcal/mol. A first important point we have to mention is that we are in a situation where the exact wavefunctions for both the thiophene and the Li–thiophene molecular systems have a strong mono-configurational character. This point is crucial for both theoretical approaches. For the CCSD(T) case it means that we do not need to resort to a multiconfigurational variant of the coupled cluster approach and thus avoid extremely expensive calculations. For the FN-DMC case, the mono-configurational character implies that the nodal patterns of the wavefunctions employed are expected to be of good quality, a point that we shall comment further later. In the case of CCSD(T) calculations the main source of error of the calculations is the use of a finite basis set associated with a maximum orbital quantum number $l$. When dynamic correlation effects are strong as in the present case, the convergence as a function of $l$ is far from being guaranteed. We stress again that the largest CCSD(T) calculations that can be done are with the AVTZ basis set (356 atomic functions and $l_{\max} = 3$). To go much further is beyond present-day computational capabilities. Now, when looking at the behavior of the BSSE-corrected values of the IE as a function of the basis set size (see Table 2), it is clear that it is difficult to conclude on the validity of the final value of $-7.5$ kcal/mol. Regarding the FN-DMC calculations, we consider that the situation is less confusing. As already noted in Sect. 3.2 the only error left in FN-DMC when statistical fluctuations have been sufficiently reduced by making long enough simulations is the fixed-node error. Here, the final statistical error is about 1.7 kcal/mol, so that it can be considered sufficiently small for correctly discriminating between the CCSD(T) and the FN-DMC results (a difference of about 9 kcal/mol). Accordingly, we just need to focus on the systematic fixed-node error, which is directly related to the quality of the nodes of the trial wavefunction employed. Numerical experience during the past 20 years has shown that there seems to be a close relationship between the multi-configurational character of the exact wavefunction and the topology of the nodal pattern [36]. When the wavefunction is multi-configurational, the Hartree–Fock nodes are usually bad. To give an illustrative example, in a recent calculation of the dissociation barrier of the $O_4$ molecule dissociating into two triplet $O_2$ molecules [37] it has been found that "mono-configurational" nodes issued from a HF calculation give a barrier of about 26 kcal/mol, while "multi-configurational" CASSCF-nodes lead to about 11 kcal/mol (more than two times smaller!), a value close to the benchmark ACPF/AVTZ multireference one. On the other hand, when the wavefunction is essentially mono-configurational it has been systematically observed that FN-DMC results obtained with Hartree–Fock-like nodes are usually good [38]. In the FN-DMC applications presented in this work, we have already noticed that all the wavefunctions have a strong monoconfigurational character. Accordingly, it is reasonable to have some confidence in the FN-DMC converged value and to conclude that the LiT complex is essentially unbound. A last point which deserves to be mentioned is the possible role played by our particular choice for the nuclear geometries. As mentioned earlier, all geometries used here for the FN-DMC simulations are those optimized at the MP2/AVTZ level (which are nearly unchanged when using the much larger AVQZ basis sets). It is clear that it would have been much more satisfactory to use the optimal nuclear geometries of each approach, in this case the FN-DMC optimized geometries for T and LiT. This is particularly important here since we have seen that there exists a strong rearrangement of the atoms of the thiophene ring when doping the system with the valence electron of the Li atom and, thus, the important dynamical correlations effects introduced by CCSD(T) or FN-DMC are expected to be strongly coupled to the nuclear geometry aspects. Unfortunately, geometry optimization with FN-DMC is still in infancy [39, 40] and no stable and robust algorithm exists up to now. Regarding CCSD(T) with very large basis sets, geometry optimizations are known to be too expensive in practice and are completely out of reach in this case.

### 6.4 Changes in electron pairing of the thiophene under electronic doping

In this section we propose to visualize the change in electron pairing of the thiophene ring when doped by the electron brought by the lithium atom. To do that we have employed the Electronic Pair Localization Function (EPLF) presented in detail in Sect. 4. Thanks to EPLF we have at our disposal a unique tool for examining the *local* electron pairing. Let us insist that since the EPLFs have been calculated at the FN-DMC level (both for the thiophene and for the LiT systems) and that the trial wavefunctions are expected to have a "good" nodal pattern (Hartree–Fock nodes for nearly-monoconfigurational wavefunctions as discussed above) the FN-DMC densities from which the EPLF electron pairings are extracted are supposed to be of a quite good quality. This remark has to be contrasted with what happens with alternative tools found in the literature such as, e.g., the ELF method [15, 16] or the AIM (Atoms In Molecules) approach [13], which is usually based on much less accurate densities (for example, using Kohn Sham orbitals).

Figures 2 and 3 present the EPLF for the thiophene ring without the lithium atom. The contours of the EPLF are

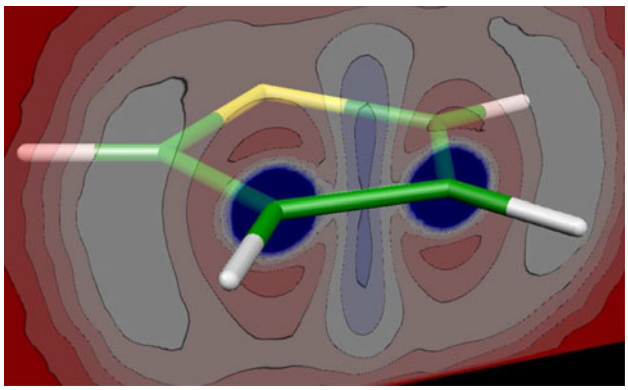

**Fig. 2** Contour plot of the EPLF of thiophene in a plane perpendicular to the two symmetry planes of the molecule and containing two carbon atoms

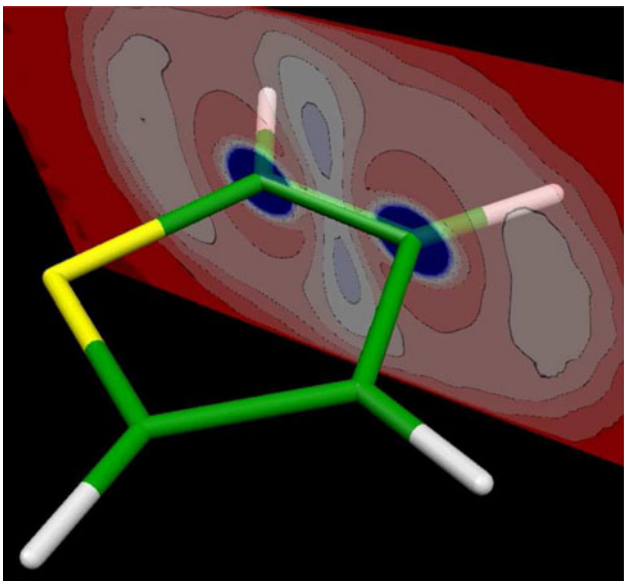

**Fig. 3** Contour plot of the EPLF of thiophene in a plane different from the plane of Fig. 2, perpendicular to the molecular plane and containing two bonded carbon atoms

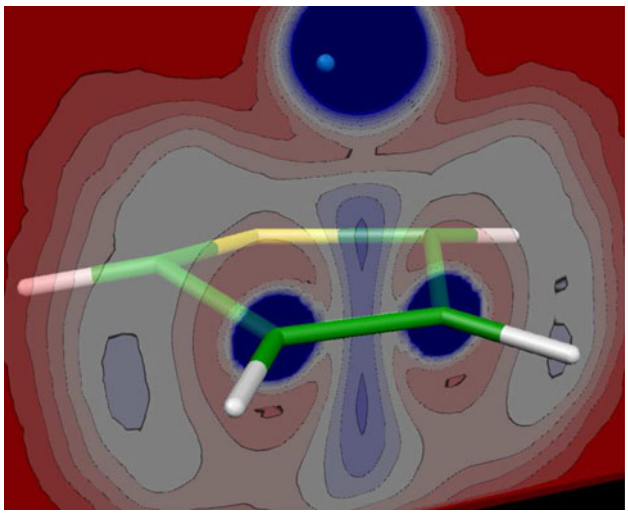

**Fig. 4** Contour plot of the EPLF of LiT in a plane analogous to the plane of Fig. 2

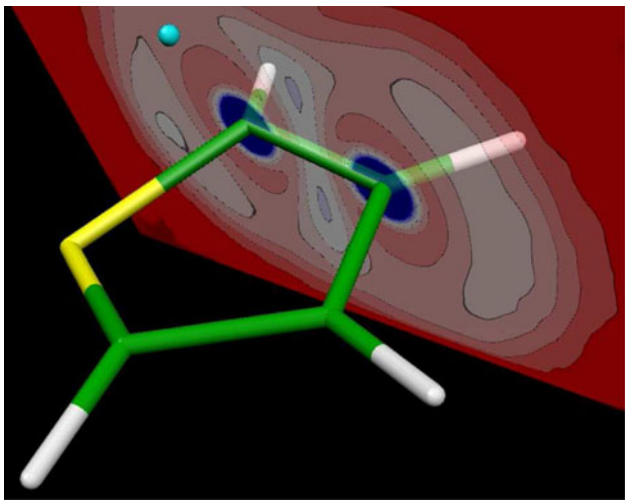

**Fig. 5** Contour plot of the EPLF of LiT in a plane analogous to the plane of Fig. 3

displayed in two different planes perpendicular to the molecular plane in order to identify the nature of the bonding between the two types of carbon–carbon bonds.

The two figures show a different EPLF topology for the two types of C–C bonds. In Fig. 2 we look at the central C–C bond (the bond opposite to the sulphur atom). For this bond the maximum of EPLF is located on the C–C axis, which is typical of a single bond. However, it can be observed that there are some high EPLF values (slightly smaller than the maximum on the axis) in domains located on both sides of the molecular plane, thus indicating an additional weak double-bond character. For the other C–C bond, Fig. 3, the EPLF has clearly two domains of maxima located on both sides of the molecular plane, a pattern typical of a double bond. Let us emphasize that the EPLF allows very easily to discriminate between different localization/delocalization regimes. Here, if the electrons were strongly delocalized between the various bonds, these two C–C bonds would be equivalent, and this would immediately appear in the EPLF figures. Clearly, the $\pi$ electrons are here not well delocalized over the three C–C bonds of thiophene.

Figures 4 and 5 display the contours of the EPLF for LiT in the two planes equivalent to those used in Figs. 2 and 3. Of course, in the presence of the lithium atom the thiophene ring is no longer planar and the planes considered are slightly different. In both figures one can see that the EPLF, in both C–C bond regions, present two domains of maxima corresponding to a strong double-bond

character. As opposed to the isolated thiophene, the topology of the three C–C bonds is now much more similar. Accordingly, it can be concluded that the electron delocalization between the three carbon bonds is much stronger in LiT than in thiophene alone. This result beautifully exemplifies the fact that by injecting an electron in the thiophene ring, the electronic structure of the doped system is *qualitatively* changed.

## 7 Summary

To summarize, the purpose of this work was essentially to get a precise evaluation of the IE of the Li–thiophene charge transfer complex by using highly correlated electronic structure calculations. This study follows previous works [8, 9] which have shown that such a task is far from being trivial, essentially due to the charge transfer occurring from the atom to the ring, which induces (mainly) significant carbon–carbon bond distance rearrangements. To understand and to quantify such effects is of great interest since the Li–thiophene system can be considered as the elementary building block of doped polythiophene polymers, which are themselves viewed as prototype systems for many technological applications (the so-called "plastic electronics"). Apart from the MP2 calculations, which have been used for geometry optimizations with all the basis sets reported here, the two very accurate methods employed in this work are the ab initio CCSD(T) approach with very large basis sets and the FN-DMC method. Note that for both approaches we are in a favorable situation since the wavefunctions of the fragments, Li, thiophene, and of the Li–thiophene molecular systems have a very strong mono-configurational character. For the CCSD(T) calculations we have found a poor convergence of the IE as a function of the basis set size. Our "best" estimate for the IE obtained with the largest basis set (AVTZ) is −7.5 kcal/mol (after correction of the BSSE), a result which is not easy to trust, despite the large-scale calculation involved (the CCSD(T)/AVTZ calculations for LiT involve about $1.5 \times 10^7$ CSF). For the FN-DMC case, these quite extensive (benchmark) calculations lead to a quite different result, since the IE found is $+1.3 \pm 1.7$ kcal/mol, which essentially means that the Li–thiophene system is unbound or perhaps is a metastable complex, due to the Repulsive Coulomb Barrier (RCB) that might prevent the complex from spontaneous dissociation. In the FN-DMC approach, the only error left at the end of the calculation (apart from the statistical error, which has been controlled here) is the fixed-node error related to the quality of the nodes of the trial wavefunction employed. The fact that the molecular systems studied have a strong mono-configurational character implies that the nodal patterns are expected to be of a rather good quality. Nevertheless, although this benchmark FN-DMC value is probably the most reliable result for the IE obtained so far, we must emphasize the current contradictory results obtained by two state-of-the-art methodologies to address this very complex interaction. From the usual ab initio perspective, standard extrapolation techniques are useless here since they require data displaying a certain level of convergence. In the case of the large fluctuations observed here for the BSSE-corrected CCSD(T) interaction energy (3.1 kcal/mol difference from the AVDZ to AVTZ values, or a 70% relative increase), extrapolation techniques would require a few additional values for larger basis sets, at the very least, the CCSD(T)/AVQZ value; however, as stated earlier, even these calculations are not feasible with the present resources. Therefore, we must wait until substantially larger computational resources are available to provide a definitive answer to the problem.

**Acknowledgments** M. Caffarel and A. Scemama would like to thank IDRIS (CNRS, Orsay), CCRT (CEA/DAM, Ile-de-France), CALMIP (Université de Toulouse) for computational support. A. Ramírez-Solís wishes to thank the FOMES2000 "Cómputo Científico" Project for CPU time on the IBM-p690 supercomputer.

## References

1. Skotheim TA (ed) (1986) Handbook of conducting polymers, vols I, II. Dekker, New York
2. McGehee MD, Miller EK, Moses D, Heeger AJ (1999) In: Bernier P et al (eds) Advances in synthetic metals: twenty years of progress in science and technology. Elsevier, Amsterdam
3. Frommer JE, Chance PR (1986) Encyclopedia of polymer science and engineering. Wiley, New York
4. Heeger AJ, Kivelson S, Schrieffer JR, Su WP (1988) Rev Mod Phys 60:781
5. Brédas J-L, Chance RR (1990) Conjugated polymeric materials: opportunities in electronics, optoelectronics and molecular electronics. NATO-ASI Series E182. Kluwer, Dodrecht
6. Brédas J-L, Silbey R (1991) Conjugated polymers: the novel science and technology of highly conducting and nonlinear optically active materials. Kluwer, Dordrecht
7. Brédas J-L, Themans B, Fripiat JG, André JM, Chance RR (1984) Phys Rev 29:6761
8. Ramírez-Solís A, Kirtman B, Bernal R, Zicovich-Wilson CM (2009) J Chem Phys 130:164904
9. Irle S, Lischka H (1995) J Chem Phys 103:1508
10. Dunning TH (1989) J Chem Phys 90:1007
11. Baker J, Nobes RH, Radom L (1986) J Comput Chem 7:349
12. Coppens P, Hall MB (eds) (1982) Electron distributions and chemical bonds. Plenum, New York
13. Bader RFW (1990) Atoms in molecules: a quantum theory. Clarendon, Oxford
14. Gadre SR, Kulkarni SA, Shrivastava IH (1992) J Chem Phys 96:5253
15. Becke AD, Edgecombe KE (1990) J Chem Phys 92:5397
16. Silvi B, Savin A (1994) Nature 371:683–686
17. Scemama A, Chaquin P, Caffarel M (2004) J Chem Phys 121:1725

18. Amador-Bedolla C, Salomón-Ferrer R, Lester WA, Vázquez-Martínez JA, Aspuru-Guzik A (2007) J Chem Phys 126:204308
19. Scemama A, Caffarel M, Ramírez-Solís A (2009) J Phys Chem A 113:9014
20. Frisch MJ, Trucks GW, Schlegel HB, Scuseria GE, Robb MA, Cheeseman JR, Zakrzewski VG, Montgomery JJA, Stratmann RE, Burant JC, Dapprich S, Millam JM, Daniels AD, Kudin KN, Strain MC, Farkas O, Tomasi J, Barone V, Cossi M, Cammi R, Mennucci B, Pomelli C, Adamo C, Clifford S, Ochterski J, Petersson GA, Ayala PY, Cui Q, Morokuma K, Rega N, Salvador P, Dannenberg JJ, Malick DK, Rabuck AD, Raghavachari K, Foresman JB, Cioslowski J, Ortiz JV, Baboul AG, Stefanov BB, Liu G, Liashenko A, Piskorz P, Komaromi I, Gomperts R, Martin RL, Fox DJ, Keith T, Al-Laham MA, Peng CY, Nanayakkara A, Challacombe M, Gill PMW, Johnson B, Chen W, Wong MW, Andrés JL, Gonzlez C, Head-Gordon M, Replogle ES, Pople JA (2002) Gaussian 98 Revision A.11.3. Pittsburg, USA
21. Hammond BL, Lester WA Jr, Reynolds PJ (1994) Monte Carlo methods in ab initio quantum chemistry. World Scientific Lecture and Course Notes in Chemistry, vol 1
22. Schmidt KE, Moskowitz JW (1990) J Chem Phys 93:4172
23. Assaraf R, Caffarel M (2000) J Chem Phys 113:4028
24. Umrigar CJ, Wilson KG, Wilkins JW (1988) Phys Rev Lett 60:1709
25. Scemama A, Leliévre T, Stoltz G, Cancés, Caffarel M (2006) J Chem Phys 125:114105
26. Flad HJ, Caffarel M, Savin A (1997) Quantum Monte Carlo calculations with multi-reference trial wave functions. Recent advances in quantum Monte Carlo methods. World Scientific Publishing, Singapore
27. Grossman JC (2004) J Chem Phys 117:1434
28. Manten S, Lüchow A (2001) J Chem Phys 115:5362
29. Pople JA, Head-Gordon M, Fox DJ, Raghavachari K, Curtiss LA (1989) J Chem Phys 90:5622
30. Assaraf R, Caffarel M (2000) J Chem Phys 113:4028
31. Filippi C, Umrigar CJ (1996) J Chem Phys 105:213
32. Clementi E, Roetti C (1974) Atomic Data and Nuclear Data Tables 14:177
33. Manten S, Lüchow A (2001) J Chem Phys 115:5362
34. Casado J, Hernández V, Hotta S, López-Navarrete JT (1998) J Chem Phys 109:10419
35. Davidson ER, Hagstrom SA, Chakravorty SJ, Meiser Umar V, Froese Fischer C (1991) Phys Rev A 44:7071
36. Bouabça T, Caffarel M, Ben Amor N, Maynau D (2009) J Chem Phys 130:114107
37. Caffarel M, Hernández-Lamoneda R, Scemama A, Ramirez-Solis A (2007) Phys Rev Lett 99:153001
38. Caffarel M, Assaraf R, Khelif A, Scemama A, Ramirez-Solís A (2006) In: Lebris C, Esteban M, Scuseria G (eds) Mathematical and numerical aspects of quantum chemistry problems. Mathematisches Forschunginstitut Oberwolfach Report 47, 7
39. Filippi C, Umrigar CJ (2000) Phys Rev B 61:R16291
40. Assaraf R, Caffarel M (2003) J Chem Phys 119:10536